Supplemental Data

Ecology of Microbial Invasions: Amplification Allows Virus Carriers to Invade More Rapidly When Rare

Sam P. Brown, Ludovic Le Chat, Marianne De Paepe, and François Taddei

Supplemental Experimental Procedures

Parameter Estimation

Because the competition experiments were performed with serial dilutions and bacterial physiology changes with density [S1], the parameters used in our models may not be constant during our experiments. Parameterizing the models with values derived in either the exponential or the stationary phase made no change to the qualitative conclusions presented in this manuscript (Figure S3). A better quantitative fit was found with values derived from stationary-phase conditions, under which cells spent most of their time during our experiments.

Carrying Capacity

Carrying capacity (k) was determined by counting the density of colony-forming units (CFU) of pure susceptible cells at stationary phase: $k = 2 \times 10^9 \pm 0.2 \times 10^9$ bacteria/ml.

Maximum Growth Rate (r)

Maximum growth rate (r) was determined by fitting an exponential curve to the first 6 hr of individual culture growth of our two susceptible strains, thus including the bacterial lag period to simplify the model: $r = 1.1 \pm 0.04$/hr.

Phage Mortality Rate (u)

Phage mortality rate (u) was determined by incubating phage populations at 37°C in "exhausted" Luria-Bertani (LB) medium (centrifuged and filtered 24 hr MG1655 susceptible culture) over a period of days and repeatedly measuring phage number. u was calculated by fitting an exponential curve to the decay of the free phage. We have determined that $u = 4.4 \times 10^{-3} \pm 3.5 \times 10^{-4}$/hr.

Phage Adsorption Constant (a) during Stationary Phase

The phage adsorption constant (a) during stationary phase was determined by mixing a 24 hr MG1655 susceptible culture and phage Φ80 to ensure a multiciplicity of infection (MOI) of 10^{-4}. The mix tubes were incubated at 37°C. Mix tubes were taken repeatedly during a period of several minutes and were centrifuged for 1 min at maximum bench centrifuge speed. One hundred milliliters of supernatant were mixed with 100 ml MG1655 susceptible overnight culture and 3 ml of Top Agar (7 g/liter) and then poured on LB plates. Thus we estimated the free-phage population at different times after phage-bacteria contact. a was calculated by fitting an exponential curve to this free-phage population and the following formula: a = (exponential fit – u) / (bacterial number in 10 ml). We have determined that $a = 3.5 \times 10^{-10} \pm 1.7 \times 10^{-10}$ per bacterium per ml per hr.

Burst Size and Latency Rate during Stationary Phase

Burst size (y) and latency rate (l) during stationary phase were determined by putting a 24 hr MG1655 37°C culture on ice for 10 min, centrifuging, and then resuspending the bacterial culture in minimal medium (M9) and mixing with phage (MOI = 0.01) for 7 min. The mix was then diluted in "exhausted LB" (centrifuged and filtered 24 hr MG1655 susceptible culture) and incubated at 37°C. Samples were taken repeatedly throughout time and mixed with 100 ml MG1655 susceptible overnight culture and 3 ml of Top Agar (7 g/liter) and then poured on LB plates. Plaque-forming units (PFU) were counted. The latent period was defined as the time until 50% of the maximum phage count was observed, and hence latency rate was determined by the number of latent periods per hr. The burst size is the factor between maximum phage number and initial phage number. We have determined that $y = 16 \pm 1$ phage and $l = 0.35 \pm 0.01$/hr.

Lysogenization Frequency during Stationary Phase

Lysogenization frequency (g) during stationary phase was determined by using Φ80 carrying kanamycin resistance (three independent clones constructed by miniTn10Kan transposition). Ten million susceptibles (from 24 hr culture) were put in contact with 10^7 Φ80(Kan^R) in 1 ml of exhausted LB during 30 min at 37°C. After this incubation, the mix was centrifuged, the supernatant removed, and 1 ml of $MgSO_4$ 10 mM added. This mix was then centrifuged, the supernatant removed, and 1 ml of $MgSO_4$ 10 mM added. Then, 100 ml was plated on LB + kanamycin where the CFU determined the density of lysogenized bacteria. One hundred milliliters were mixed with 100 ml MG1655 susceptible overnight culture and 3 ml of Top Agar (7 g/liter) and then poured on LB plates. The PFU determined the density of nonlysogenized infected bacteria. The lysogenization frequency during stationary phase is g = (lysogenized bacteria)/(lysogenized bacteria + nonlysogenized bacteria). We have determined that $g = 2.3 \times 10^{-3} \pm 4.5 \times 10^{-4}$ per infected bacterium.

Induction Rate during Stationary Phase

Induction rate (x) during stationary phase was determined by diluting stationary lysogenic strain culture in exhausted-LB medium to obtain samples of approximately 100 bacteria per 1 ml tube. After 4 hr of growth (37°C, LB) CFU was determined for three tubes and PFU for the remaining 77 tubes. The proportion of tubes with zero PFU allowed an estimation of the mean number of bursts per tube, under the assumption that burst events are randomly distributed (Poisson distribution). Several tubes presented nonzero PFU; in these tubes, one or more bacteria had been induced and x was determined by the following formula: x = (total number of inductions per hr / total number of bacteria) = (number of tubes with nonzero PFU × mean number of bursts per tube × 60/69) / (number of tubes (77) × number of bacteria at beginning × number of generation in 69 min (4 hr − 171 min of latency)). We have $x = 3.7 \times 10^{-3} \pm 1.5 \times 10^{-3}$ per lysogenized bacterium per hr.

Protocols for phage mortality rate and phage adsorption constant were adapted from [S2]. Protocols for burst size and latency rate were adapted from [S3], and protocols for induction rate were adapted from [S4].

Population Dynamics of Phage-Mediated and Bacteriocin-Mediated Competition

Phage-Mediated Competition

We model the dynamics of phage-carrying and susceptible strains by using a system centered on three interacting populations: the densities of the phage-carrier strain, C; the susceptible uninfected strain, S; and free phage, V (our models are variants on models presented in [S5–S9]). To improve the temporal fit, we add the dynamics of latent cells, L, which are carriers or infected susceptibles that are about to lyse. To illustrate the separate interests of bacteria and phage, we track separately the newly derived carriers, C^S, which are lysogenized susceptibles made immune to further infection because of the integration of the phage into the host genome (see right diagram in Table 1):

$$\begin{aligned} dC/dt &= (r(1 - N/k) - x)C \\ dS/dt &= (r(1 - N/k) - aV)S \\ dC^s/dt &= (r(1 - N/k) - X)C^s + gaVS \\ dL/dt &= x(C + C^s) + (1 - g)aVS - lL \\ dV/dt &= ylL - V(u + aN) \end{aligned} \quad (1)$$

The bacterial strains C, C^S, and S have the same maximum rate of increase, r, and carrying capacity, k, but the carrier lineages C and C^S suffer an additional loss, with x representing the rate of phage-induced lysis. Probabilistic phage-mediated death in the lysogenic lineages C and C^S results in a population of latent cells, L, that lyse at rate l, each then releasing y new free phage, augmenting the free-phage population, V. Phage-mediated killing of the nonlysogenized lineage, S, occurs at a rate determined by the adsorption parameter, a, of free phage on bacterial cells. Susceptible cells pass into one of two categories after absorption of free phage. In a small minority of

Table S1. Ascent of New Lysogens among the Initially Susceptible Lineage

Initial Carrier to Susceptible (*C*/*S*) Ratio	Time of Competition	New Lysogens to Susceptibles Ratio (*CS*/*S*)	
		Observed	Expected
1/100	36 hr	10/10	10/10
1/1	36 hr	20/20	20/20
100/1	36 hr	2/30	0.2/30
100/1	72 hr	6/30	1.9/30

Independent clones were sampled from the competition experiments at the time points indicated and were cultivated in LB medium for 8 hr. The cultures were then centrifuged (3 min, maximum bench centrifuge speed), and 10 μl of supernatants were spotted on a susceptible layer. If the supernatant contained phage (seen as lysis zone on the bacterial layer after one night), the clone from the *S* lineage was considered as having been lysogenized. *C* denotes phage carriers, *S* denotes susceptibles, and C^S denotes lysogenized derivatives of susceptibles. Please note that as expected from the model (model and parameters as for Figure 1, no significant difference with observed values, corrected Chi-squared $p > 0.25$ for each line), the initially susceptible lineage can persist in a lysogenized form.

cases, determined with a probability $g << 1$, the phage lysogenizes within its new host, creating a population of lysogens derived from *S*, C^S (given our assumption of no intrinsic differences between the invasive carrier lineage, *C*, and the resident susceptible lineage, *S*, the "original" and newly derived carriers *C* and C^S are functionally equivalent, although of different bacterial lineage). However, in the large majority $(1 - g)$ of cases, when a free phage successfully binds a susceptible cell, the phage exploits the new host cell lytically, leading to new latent cells and ultimately new free phage. Free phage die with a mortality rate (u) or irreversibly adsorb onto viable cells N ($N = C + S + C^S$). Model 1 underlies the simulation results presented in Figures 1, S1, and S3, together with the stability analysis of phage-mediated competition (red line) in Figure 3B. Note that our model ignores segregation of the prophage during vertical transmission (a potential ongoing source of *S* cells derived from a C^S lineage), as well as phage-resistant nonlysogens or lytic virulent phage mutants.

Model 1 has three equilibria that are potentially stable for positive parameter values: a susceptible-only equilibrium $\{S = k, C = C^S = L = V = 0\}$; an *S*, *L*, *V*, and C^S present equilibrium $\{C = 0, S = u(ru - ak(r - x)(y - 1))/a(y - 1)[ru(1 - g) + ak(x - r(1 - g))(y - 1)], L = ru(ak(y - 1) - u)/a^2kl(y - 1)^2, V = r(ak(y - 1) - u)/a^2k(y - 1), C^s = gru(ak(y - 1) - u)/a(y - 1)[ru(1 - g) + ak(x - r(1 - g))(y - 1)]\}$; and a susceptible-excluded equilibrium $\{C + C^s = k(1 - x/r), S = 0, L = kx(r - x)/lr, V = kxy(r - x)/ru + ak(r - x)\}$. A stability analysis reveals that the susceptible-excluded equilibrium is the only stable and attainable equilibrium whenever $k > ru/a(r - x)(y - 1)$. Thus for high densities as found under our experimental conditions, the phage/phage-carrier partnership always wins, irrespective of initial frequency. The line $k = ru/a(r - x)(y - 1)$ is approximated for our experimental conditions by the red line in Figure 3B. The analytic stability conditions for the remaining potential equilibriums are more complicated in the full model; however, for the limiting case of $g = 0$, we find that the susceptible-only equilibrium is stable whenever $k < u/a(y - 1)$. Thus for sufficiently low densities, neither the free phage nor the phage-carrying lineage can successfully invade. The line $k = u/a(y - 1)$ is also approximated for our experimental conditions by the red line in Figure 3B, because when $r >> x$, the frontiers to the susceptible-only and susceptible-excluded equilibriums converge on $k = u/a(y - 1)$. A numerical stability analysis with the observed $g = 0.0023$ confirms the above results within the resolution of Figure 3B and further illustrates that in the narrow band of cell densities $u/a(y - 1) > k > ru/a(r - x)(y - 1)$, the *S*, *L*, *V*, and C^S present equilibrium is the sole stable and attainable equilibrium. In this narrow band (lost within the red line in Figure 3B, because $r >> x$), the free phage are able to coexist with susceptibles whereas initial carriers (*C*) are driven to extinction as a result of the cost of lysis (x). However, new C^S are constantly formed by lysogenization of susceptibles, although subsequently outcompeted by *S*.

Colicin-Mediated Competition

By suppressing lysogenization and phage amplification on susceptibles, we can contrast model 1 with a model of colicin-mediated competition (see left diagram in Table 1):

$$\begin{aligned} dC/dt &= (r(1 - N/k) - x)C \\ dS/dt &= (r(1 - N/k) - aV)S \\ dL/dt &= xC - lL \\ dV/dt &= ylL - V(u + aN) \end{aligned} \quad (2)$$

Model 2 also has three equilibriums that are potentially stable for positive parameter values: a susceptible-only equilibrium $\{S = k, C = L = V = 0\}$; an all-present equilibrium $\{C = ak(r - x) + ru/ary, S = ak(r - x)(y - 1) - ru/ary, L = x(ak(r - x) + ru)/alry, V = x/a\}$; and a susceptible-excluded equilibrium $\{C = k(1 - x/y), S = 0, L = kx(r - x)/lr, V = kxy(r - x)/ru + ak(r - x)\}$. Note that the susceptibles-excluded equilibrium is identical to the susceptibles-excluded equilibrium for the phage model, reflecting the convergence of phage-mediated competition on the nonmultiplicative colicin model when susceptibles become increasingly scarce. In contrast to the phage model, however, the susceptibles-only solution is always locally stable for positive parameters. Thus for parameter values universally favoring phage carriers, the colicin model displays two locally stable equilibriums, with the exclusion or fixation of susceptibles depending on their initial frequencies (Figure 3B [S7, S8],). In contrast to previous studies, we in addition show that this frequency threshold decreases

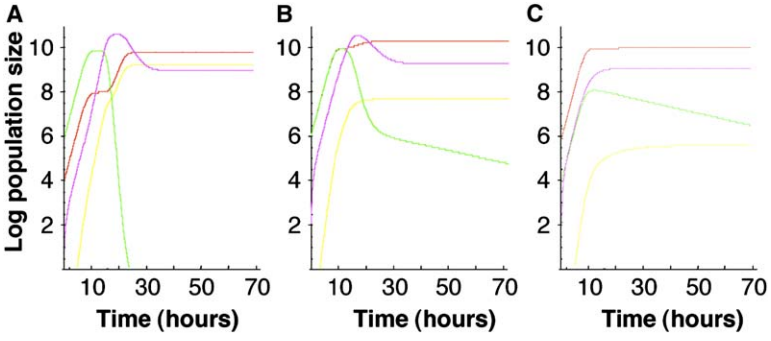

Figure S1. Simulated-Competition Results

Simulated temporal dynamics of densities of phage carrier (*C*, red), susceptible (*S*, green), lysogenized derivative of *S* (C^S, yellow), and phage particle (*V*, pink) given initiation with (A) $C = 10^3$ nd $S = 10^5$; (B), $C = S = 10^5$, and (C) $C = 10^5$, $S = 10^3$. C^5 and *V* have zero initial densities throughout. Parameters and model are as for Figure 1 (panels [A], [B], and [C] correspond to red, blue, and green lines, respectively, in Figure 1).

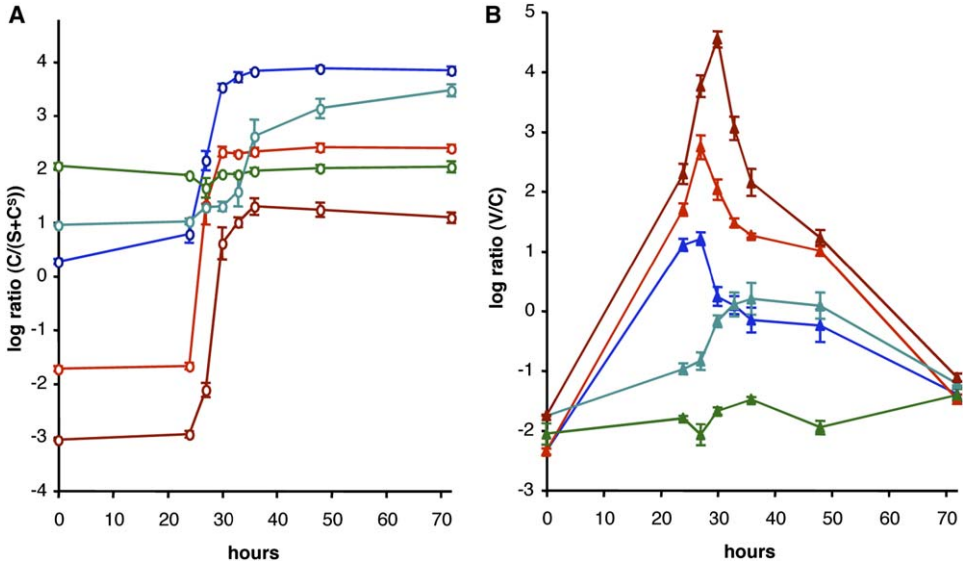

Figure S2. Experimental-Competition Results

(A) Ratio of phage carriers to susceptibles and lysogenized susceptibles.

(B) Ratio of free phage to carriers. Data points are the mean of six replicates, three with one coupling of two antibiotic markers and three with the reverse coupling. Populations of susceptibles and lysogenized derivatives of susceptibles were followed by monitoring the antibiotic-resistant population; thus we do not distinguish between them. Error bars represent standard errors of the mean (sometimes hidden by the symbols).

with total bacterial abundance, illustrating that the success of bacteriocins should be viewed as both frequency- and density-dependent (Figure 3B). The frequency threshold to carrier invasion is defined by the repelling all-present equilibrium, yielding a threshold of $ak(r-x)+ru/aky(r-x)$. When $C/N > ak(r-x)+ru/aky(r-x)$, carriers go to fixation; otherwise, susceptibles go to fixation. This threshold is illustrated for the observed nonreplicating phage by the black line in Figure 3B. Note that we see clearly that for increasing density (higher k), the frequency threshold approaches a constant nonzero value, i.e., the rarity threshold is inescapable. The asymptote is simply $1/y$—the more weapons produced per lysed cell, the lower the limiting threshold to invasion. In contrast, when $k < ru/a(r-x)(y-1)$, 100% carriers cannot resist susceptible invasion. As carrying capacity declines, loss of the chemical weapon (degredation, aggregation, inappropriate binding, etc.) becomes increasingly significant until a threshold is reached where a pure population of carrier cells can no longer defend themselves against susceptibles.

Contrasting Phage- and Colicin-Mediated Competition

Whereas phage can act essentially as a colicin-style nonmultiplicative killer when their carriers are numerically dominant, they are likely to do so in a less efficient manner because of their relatively wasteful capacity for replication (e.g., estimates of effective colicin "burst size" are far greater than figures reported in this study for temperate

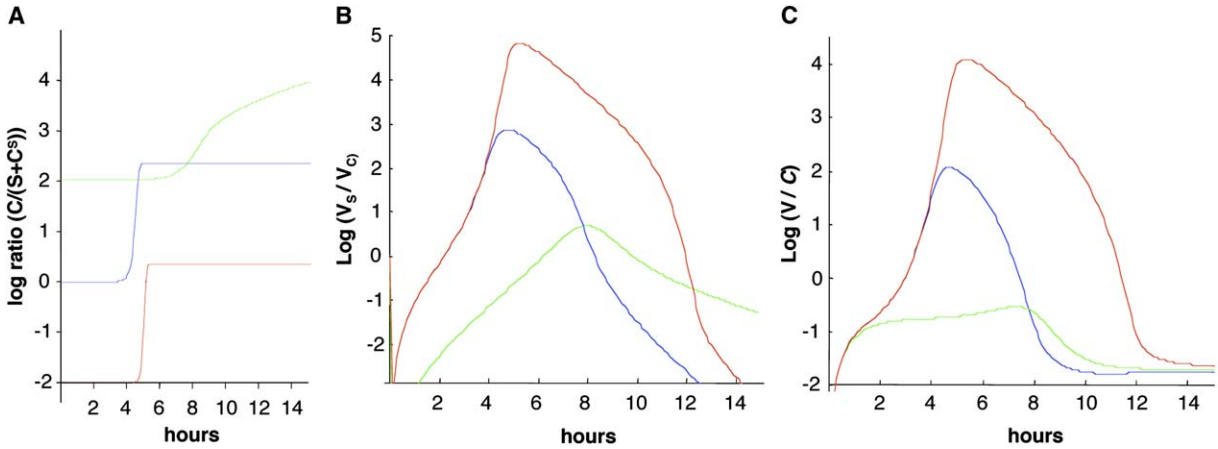

Figure S3. Simulated Competition with Exponential Phase Parameters

C denotes phage carriers, S denotes susceptibles, and C^S denotes lysogenized derivatives of S. For all initial ratios, the speed of attaining the final-carrier-only equilibrium is much faster than for the stationary-phase parameter set (Figure 1); however, the qualitative effects of initial ratio on relative speed remain. When carriers are initially common (green line, $C = 10^5$, $S = 10^3$), the approach to equilibrium is slower than when susceptibles are initially more abundant (blue and red lines; see also Figures 1 and 2). By exploring model behavior at the two extremes of bacterial physiology (exponential and stationary phase), we can see that the qualitative phenomenon of "faster killing with susceptible abundance" is a robust phenomenon, plausible at any point in the bacterial growth cycle. The generality of this principle is clear from the dependence of the free viral reproductive number, $R = yaS/u + a(S+C)$, on the density of susceptible hosts, S (epidemic requires $S > u + aC/a(y-1)$. Parameter estimations in exponential phase were r = 1.1/hr, $k = 2 \times 10^9$ bacteria/ml, $x = 7.3 \times 10^{-4}$ per lysogenized bacterium per hr, y = 557 phage per burst, $u = 5 \times 10^{-3}$/hr, $a = 1.1 \times 10^{-8}$ per bacterium per ml per hr, l = 1.02/hr, and $g = 4.6 \times 10^{-3}$ per infected bacterium.

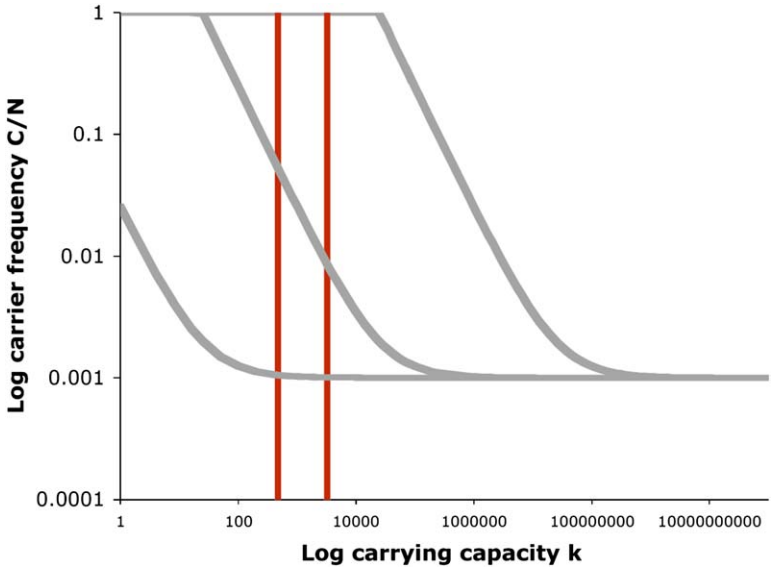

Figure S4. Stability Analyses of Chemical and Viral Competition

Equilibrium behavior as a function of bacterial density (*k*) and carrier frequency (*C/N*). The red line $(k = u/a(y-1))$ outlines virus-carrier stability, and the gray lines $(C/N = ak + u/aky)$ outline chemical-carrier stability as described in Figure 3B. The left red line indicates parameters for temperate phage P4, and the right red line indicates parameters for temperate phage P2. Gray lines are *y* and *a* estimates that represent best guesses for typical colicins (see text). Values of decay term (*u*) are (from left to right) 10^{-7}, 10^{-4}, and 0.1/hr. Note when $u = 0$, invasion of colicin carriers is purely frequency dependent (threshold 1/*y*).

phage, see below). Giving a chemical carrier an advantage in the number of lethal doses produced on the lysis of a single carrier cell (gray line, Figure 3B) leads to a region of parameter space where a chemical carrier could repel rare susceptible invaders, but a phage carrier could not (gray region—high frequency, moderate density—in Figure 3B). However, despite this production advantage for the chemical carrier, the phage carrier continues to have a unique advantage when sufficiently rare (pink region—low frequency, high density—in Figure 3B).

By making the simplifying assumptions of $r >> x$ and $g = 0$, we can reduce the stability analyses to three variables: burst size, *y*; adsorption rate, *a*; and decay rate, *u*. If we then consider that burst size (*y*) alone varies between chemical (y_c) and viral (y_v) weapons, we can note that the intersection of the red and gray lines in Figure 3B is at a frequency $C/N = y_v/y_c$. Above this frequency, there exists a region of intermediate densities $u/a(y_c C/N - 1) < k < u/a(y_v - 1)$ where a chemical weapon is the only efficient strategy of competition (gray zone in Figure 3B). Below this frequency and above the viral-density threshold $u/a(y_v - 1)$, a viral weapon is uniquely beneficial (pink zone in Figure 3B; in the limit of large *k*, the threshold becomes $C/N < 1/y_c$).

In Figure S4, we consider parameter variations in *a*, *u*, and *y*. First, we consider the phage-carrier threshold (red line, Figure 3B) for parameters measured in exponential conditions. Not surprisingly, the threshold density for phage-carrier victory is significantly lower in exponential phase, at around $u/a(y-1) \approx 8.18 \times 10^2$. We can now contrast this threshold value with thresholds calculated from published estimates of *a*, *y*, and *u* for a range of temperate phage [S10]. Across the phages Lambda, P1, P2, P4, and Φ80, we find reasonable agreement, with threshold densities varying from 4.75×10^2 (P4) to 3.26×10^3 (P2) (red lines, Figure S4). Regarding colicins, to our knowledge there are no comprehensive studies of the parameters *a*, *y*, and *u* for any given system. We tentatively estimate a typical effective burst size (number of lethal doses on lysis) as $y = 10^3$, based on reports of the number of E1 colicins released being on the order of 10^5 ([S8], K. Jakes personal communication) and the binding of on average 100 colicin molecules per lethal event [S11]. This estimate of *y* is consistent with the reported invasion threshold of $C/N \approx 10^{-2.5}$ [S12]. For adsorption (*a*), we use a guide estimate of 5×10^{-9} [S13]. Finally, the rate of intrinsic decay of colicin proteins (e.g., as a result of degredation, aggregation, inappropriate binding, etc.) is known to vary greatly in response to environmental conditions [S14, S15], so we plot the invasion threshold for varying values of intrinsic decay (*u*) (gray lines, Figure S4). We see that for sufficiently high rates of colicin degredation, a phage carrier could even outperform a colicin carrier in a defensive context.

All analyses and simulations were performed in Mathematica 4.0 (Wolfram Research, Illinois, 1994). The simulation code is available on request.

Supplemental References

S1. Huisman, G., Siegele, D., Zambrano, M., and Kolter, R. (1996). Morphological and physiological changes during stationary phase. In Escherichia coli and Salmonella, F. Neidhardt, ed. (Washington, D.C.: ASM Press), pp. 1672–1682.

S2. Adams, M.H. (1959). Bacteriophages (London: Interscience Publishers).

S3. Ekechukwu, M.C., Oberste, D.J., and Fane, B.A. (1995). Host and {phi}X 174 mutations affecting the morphogenesis or stabilization of the 50S complex, a single-stranded DNA synthesizing intermediate. Genetics *140*, 1167–1174.

S4. Bertani, G. (1951). Studies on lysogenesis. I. The mode of phage liberation by lysogenic Escherichia coli. J. Bacteriol. *62*, 293–300.

S5. Chao, L., and Levin, B.R. (1981). Structured habitats and the evolution of anticompetitor toxins in bacteria. Proc. Natl. Acad. Sci. USA *78*, 6324–6328.

S6. Levin, B.R. (1988). Frequency-dependent selection in bacterial populations. Philos. Trans. R. Soc. Lond. B Biol. Sci. *319*, 459–472.

S7. Frank, S.A. (1994). Spatial polymorphism of bacteriocins and other allelopathic traits. Evol. Ecol. *8*, 369–386.

S8. Durrett, R., and Levin, S. (1997). Allelopathy in spatially distributed populations. J. Theor. Biol. *185*, 165–171.

S9. Stewart, F.M., and Levin, B.R. (1984). The population biology of bacterial viruses: Why be temperate. Theor. Popul. Biol. *26*, 93–117.

S10. De Paepe, M., and Taddei, F. (2006). Viruses' life history: Towards a mechanistic basis of a trade-off between survival and reproduction among phages. PLoS Biol. *4*, e193.

S11. Farid-Sabet, S. (1982). Interaction of 125I-labeled colicin E1 with Escherichia coli. J. Bacteriol. *150*, 1383–1390.

S12. Joo, J., Gunny, M., Cases, M., Hudson, P., Albert, R., and Harvill, E. (2006). Bacteriophage-mediated competition in Bordetella bacteria. Proc. Biol. Sci. *273*, 1843–1848.

S13. Reynolds, B.L., and Reeves, P.R. (1969). Kinetics of adsorption of colicin CA42-E2 and reversal of its bactericidal activity. J. Bacteriol. *100*, 301–309.

S14. Brey, R.N. (1982). Fragmentation of colicins A and E1 by cell surface proteases. J. Bacteriol. *149*, 306–315.

S15. Cavard, D., Régnier, P., and Lazdunski, C. (1982). Specific cleavage of colicin A by outer membrane proteases from sensitive and insensitive strains of E. coli. FEMS Microbiol. Lett. *14*, 283–289.